Efficient Production of Mechanically Recyclable and Compostable Blown Films of Thermoplastic Starch/Poly(Butylene Succinate-Co-Adipate) Blends

Macromolecular Materials and Engineering

Macromolecular Materials and Engineering Open Access

www.mame-journal.de

RESEARCH ARTICLE OPEN ACCESS

Efficient Production of Mechanically Recyclable and Compostable Blown Films of Thermoplastic Starch/Poly(Butylene Succinate-Co-Adipate) Blends

Giulia Piciullo[1] | Angelica Avella[1,2] | Yohan Bonnard[1] | Claudio Gioia[3] | Annamaria Celli[4] | Giada Lo Re[1,2,5]

[1]Department of Industrial and Materials Science, Chalmers University of Technology, Gothenburg, Sweden | [2]Wallenberg Wood Science Center, Chalmers University of Technology, Gothenburg, Sweden | [3]Department of Physics, University of Trento, Povo, Italy | [4]Department of Civil, Chemical, Environmental and Materials Engineering, University of Bologna, Bologna, Italy | [5]Department of Civil and Industrial Engineering, University of Pisa, Pisa, Italy

Correspondence: Giada Lo Re (giadal@chalmers.se)

Received: 14 April 2026 | **Revised:** 24 May 2026 | **Accepted:** 10 June 2026

Keywords: biodegradation | extrusion | film blowing | mechanical recycling | poly(butylene succinate-co-adipate) | thermoplastic starch

ABSTRACT

Sustainable bio-based and biodegradable materials are receiving increased attention in response to the environmental impact of conventional non-biodegradable plastics. Thermoplastic starch (TPS) and poly(butylene succinate-co-adipate) (PBSA) are bio-based and biodegradable materials that have the potential to serve as an alternative solution in the disposable packaging sector. The melt processing of TPS is, however, challenging due to its moisture sensitivity and rapid aging. This study investigates the development of TPS/PBSA blends without compatibilizers, comparing a conventional two-step processing method with a one-step approach combining starch plasticization and its blending with PBSA. The one-step process exhibits higher stability, making it a promising candidate for industrial applications due to its reduced energy consumption and production costs. To contribute to waste reduction, disintegration in industrial composting and multiple cycles of mechanical recycling were performed.

1 | Introduction

Conventional fossil-based thermoplastic polyolefins, including polyethylene (PE) and polypropylene (PP), are the most produced polymers and possess a high degree of durability [1]. However, they are not biodegradable, which results in their accumulation in landfills and marine environments when not correctly disposed of. In packaging applications, plastics have limited service life and are predominantly disposed of rather than reused or recycled. It is estimated that approximately 60% of all plastic ever produced has been landfilled [1], with only a small fraction being recycled or reused [1, 2]. In response to the global challenge of reducing plastic waste, there has been a growing interest in thermoplastic bio-based materials. When designed to be recyclable or biodegradable, these materials can be a sustainable alternative to conventional packaging plastics [3]. Several biodegradable thermoplastics, derived from petroleum or renewable resources, are currently on the market, including poly(lactic acid), poly(butylene adipate-co-terephthalate) (PBAT) and poly(butylene succinate-co-adipate) (PBSA). However, these materials still have a higher cost than conventional PE or PP [4]. To address this limitation, a promising strategy involves the incorporation of low-cost agricultural by-products into higher-cost biodegradable polymers. This would lower production costs and support the principles of circular bioeconomy [5].

Starch is a natural polymer that can be transformed to thermoplastic starch (TPS) through plasticization processes that modify its structure. Once plasticized, TPS can be melt-processed similarly to synthetic plastics, using common techniques such as extrusion or injection molding. Due to the inherent moisture sensitivity and rapid aging, it is often necessary to blend TPS

with other thermoplastics to ensure stable processing and product performance [6]. Examples of TPS blends with synthetic non-biodegradable polymers, like PE, have been reported in the literature [7–9]. However, these blends cannot be sorted as biological waste. A few starch-based blends, like Mater-Bi (Novamont, Italy) and Bioplast (Biotec, Germany), are commercially available [10], but are still not competitive with oil-based polyolefins.

Among the alternative biopolymers, bio-based PBSA stands out due to its mechanical properties, including flexibility, toughness, and water resistance, although presenting relatively low biodegradation kinetics. For example, in activated sludge soil it degrades by 69 wt.% in 55 days [11]. Despite its potential, few studies have investigated starch/PBSA blends, particularly with respect to process scalability or the design of manufacturing methods for compostable films. Ratto et al. [12] investigated the processing, performance, and biodegradability of blends made of starch granules embedded in a PBSA matrix by blown film extrusion. Incorporating starch up to 30 wt.% resulted in increased modulus but decreased tensile strength, strain at break, and toughness. Nevertheless, the mechanical properties remained within a suitable range for applications such as trash bags. Biodegradation tests in soil demonstrated that adding 5 wt.% starch reduced the half-life of PBSA from 231 days (pure PBSA) to 80 days. TPS has also been investigated in the production of biodegradable blends by Wang et al. [13]. In their two-step process, TPS pellets were first produced via melt compounding, then pelletized, dried, and subsequently compounded with PBSA in a twin-screw extruder (TSE). Tensile testing of injection-molded specimens revealed that TPS contents above 10 wt.% led to a progressive decline in mechanical properties. However, when TPS was evenly dispersed in the PBSA matrix at 10 wt.%, only a moderate reduction in strain at break and tensile strength was observed.

To address this challenge, the aim of our study is to develop TPS/PBSA blends without the use of compatibilizers, with a particular focus on melt processing design for film production via casting extrusion and film blowing using a single-screw extruder (SSE), relevant manufacturing techniques for packaging applications. Two distinct processing methods were compared: a two-step process and a one-step process. In the two-step process, TPS was first produced in a TSE and subsequently compounded with PBSA, under the assumption that starch plasticization would be more effective during the initial step. In contrast, the one-step process combined plasticization, blending, and film manufacturing in a SSE, offering a more cost-effective approach. By relying only on the SSE, the one-step method reduces initial industrial investment and energy consumption, therefore contributing to a more affordable and environmentally friendly processing design.

Few studies have previously compared the effect of blending processes starting from starch granules vs. thermoplastic starch [14, 15]. Brandelero et al. [14] demonstrated that a one-step process was beneficial for poly(butylene adipate-co-terephthalate) blends with high starch content (> 50 wt.%). They concluded that in the one-step approach, native starch has greater interactions with the polymer matrix compared to TPS pellets due to a larger contact area. On the other hand, Noomhorm et al. [15] indicated that the prior gelatinization of starch increased the tensile strength of blends.

In this work, the properties of the extruded blends were evaluated through tensile testing, dynamic mechanical analysis, and morphological characterization. Comparing the performance of the one-step and two-step blends provided insights into the processing–structure–property relationships, critical for selecting an appropriate manufacturing strategy. Furthermore, to assess the waste reduction potential of the developed materials, post-industrial mechanical recycling was simulated by subjecting the blends to four melt reprocessing cycles after one year of storage and subsequently evaluating the mechanical properties of the recycled material. Industrial composting was also examined as a viable end-of-life option.

2 | Materials and Methods

2.1 | Materials

Native potato starch with an amylose content of about 20% [16] was supplied by Lyckeby Stärkelsen (Sweden). Starch had a 13% equilibrium moisture content, and the glass transition temperature was 71.7°C, identified by differential scanning calorimetry (DSC) (Figure S1). The weight average (850 kDa) and number average (600 kDa) molecular weights and polydispersity (1.4) of potato starch were determined by gel permeation chromatography (GPC; Table S1). PBSA, under the name of BioPBS FD92PM, was purchased from PTT MCC Biochem Co. According to the supplier, the PBSA has a 1.24 g cm^{-3} density, a melting temperature (T_m) of 84°C, and a melt flow rate of 4 g/10 min at 190°C/2.16 kg. As reported by the supplier, the chosen PBSA grade is labeled as compostable in home and industrial conditions; moreover, it is classified as safe for food contact. Glycerol was supplied by Sigma-Aldrich (Sweden) and used as received.

2.2 | Blends Extrusion

To produce TPS-PBSA blends, two methods, indicated as one-step and two-step methods, were performed and compared in terms of processing characteristics and final properties of the prepared materials. The approach for the two methods is illustrated in Figure 1.

In the two-step method, first, TPS was produced. Starch and glycerol were manually premixed in batches with a weight ratio of 100:35. This ratio was selected based on the work by Sessini et al. [17]. Then, deionized water was added (30 wt.% of the total solids), and the mixture was sealed and stored at room temperature for 24 h. This was done to allow the absorption of the plasticizer in the starch. The plasticization was carried out in a co-rotating TSE Werner & Pfleiderer ZSK 30 M9/2 (Stuttgart, Germany), with a screw diameter of 30 mm and a screw length of 966 mm. It was equipped with six heating zones, including the external die. The temperature profile in the different zones was 80-90-100-120-130-90°C, screw speed was set to 100 rpm, and residence time was around 2 min. A screw design with 7 kneading elements was chosen to ensure good mixing (Figure S2) [18]. The temperature at the die was kept below 100°C to prevent the melt from boiling, resulting in a bubble-free extrudate [19]. A ventilation port before the die was kept open during the process to let the water evaporate. At the exit of the die, the filament was

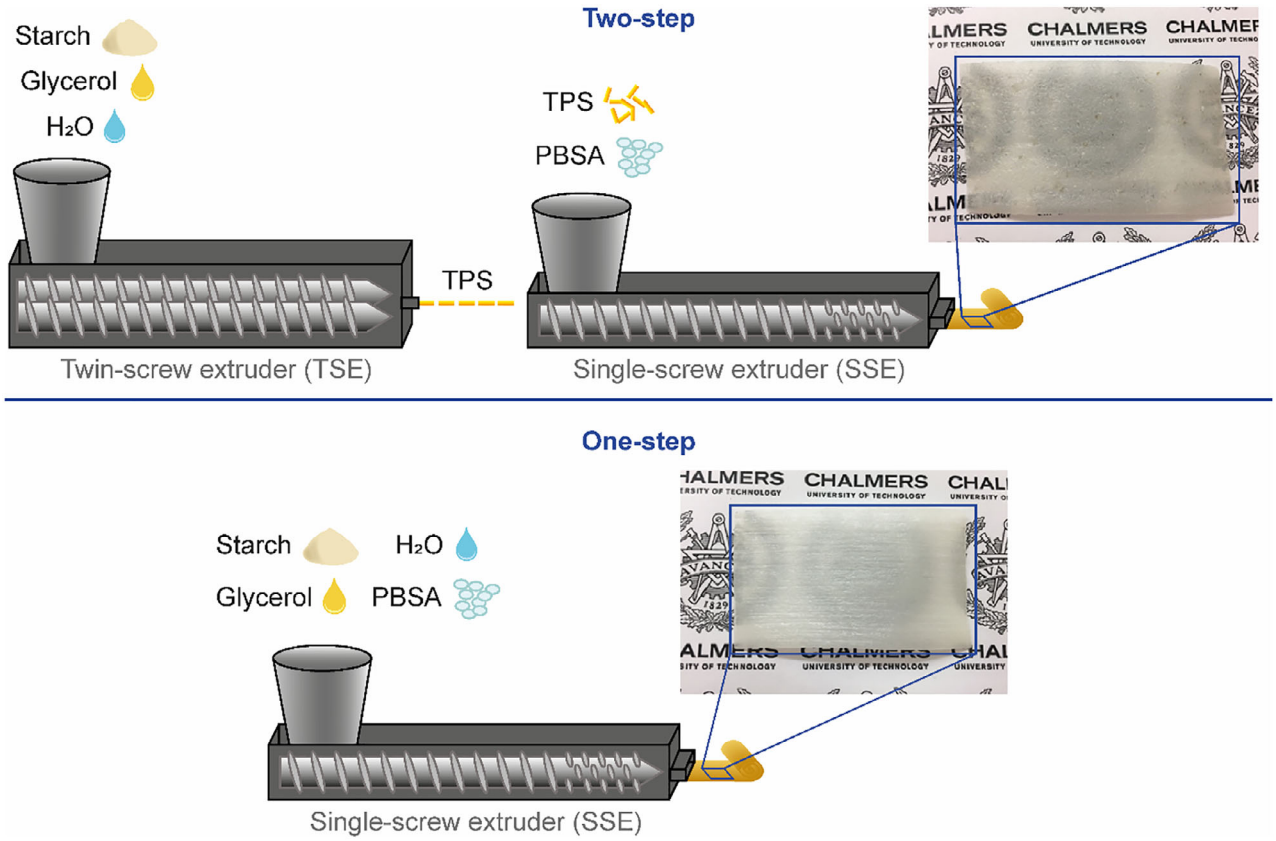

FIGURE 1 | Screw configuration and visual aspect of the blend obtained in (a) two-step and (b) one-step processes.

collected on a conveyor belt. TPS was dried at 70°C for 12 h in a ventilated oven and afterward pelletized. Finally, the blending of TPS pellets and PBSA was performed in a SSE Brabender OHG (Duisburg, Germany), with screw diameter D = 19 mm and screw length 25D. The temperature profile from hopper to die was 80-100-120-90°C, and the screw speed was 100 rpm. A barrier screw 2.5:1 with a mixing element was chosen to ensure good compounding. The residence time was between 2 and 3 min. The extruder was equipped with a flat die (50 mm width) for the production of sheets with thicknesses ranging from 50 μm to 2 mm. The TPS pellets were mixed with PBSA in the proportions shown in Table 1. The final blends are called P*XX*-T*YY* II, where the *XX* code indicates the wt.% of PBSA and the *YY* code indicates the wt.% of TPS.

For the one-step method, batches were prepared by manually mixing native starch, glycerol, deionized water, and PBSA in the ratios reported in Table 1. The batches were stored at room temperature for 24 h in sealed plastic bags. The melt extrusion of the batches was carried out in the SSE following the method described above for the PBSA/TPS blending. Manual feeding was done at a slow and constant rate. The final samples are called PZZ-THH, where the ZZ code indicates the wt.% of PBSA and the HH code indicates the sum of wt.% of native starch and glycerol.

2.2.1 | Film Blowing

The neat PBSA and the P70-T30 blend were also film-blown using the SSE equipped with a film blowing die with a cooling ring. The processing was performed in one step, 24 h after preparing the mixtures of starch, glycerol, water, and PBSA. The screw speed was 40 rpm, and the temperature profile from hopper to die was 80-100-120-100°C. The film produced was then collected and pulled by rotating rolls above the die.

2.3 | End-of-Life

2.3.1 | Mechanical Recycling

One year after their production, PBSA and the P70-T30 blown films were reprocessed up to four times, simulating a post-industrial mechanical recycling process. During the year, the materials were stored at room temperature in sealed bags. The films were first manually shredded, then the pieces were fed into an Xplore MC15 twin-screw microcompounder. The processing temperature was set to 120°C. The screw speed during feeding was 20 rpm (5 min), and 100 rpm during processing (5 min). The materials were extruded through a circular die and manually pelletized. Two batches of about 15 grams each were processed for each sample, and the pellets were manually mixed for homogeneity. Half of the mixed batch was reprocessed for three more cycles under the same conditions, amounting to a total of four reprocessing cycles per material. The materials after one and four cycles were then injection-molded into dumbbell-shaped tensile specimens (gauge length of 25 mm) using an Xplore IM12 injection molder. The barrel temperature was 120°C, and the injection and holding pressures were set to 350 and 485 bar, respectively. The shredded films were also directly injection-

TABLE 1 | Compositions of PBSA (P) and TPS (T) blends in two-step (II) and one-step extrusion.

Two-step process					
	Preparation of TPS in TSE[a]				**Preparation of blends in SSE[a]**
Material	**Native starch [wt.%]**	**Glycerol [wt.%]**	**Water[b] [wt.%]**	**TPS [wt.%]**	**PBSA [wt.%]**
P70-T30 II	74	26	30	30	70
P60-T40 II	74	26	30	40	60
P50-T50 II	74	26	30	50	50
P40-T60 II	74	26	30	60	40

One-step process				
		Preparation of blends in SSE[a]		
Material	**Native starch [wt.%]**	**Glycerol [wt.%]**	**Water[b] [wt.%]**	**PBSA [wt%]**
P70-T30	22.2	7.8	30	70
P60-T40	29.5	10.5	30	60
P50-T50	37	13	30	50
P40-T60	44.3	15.7	30	40

[a]Twin-screw extruder (TSE) and single-screw extruder (SSE).
[b]The percentage of water refers to the total solids amount fed.

molded under the same conditions to obtain reference specimens. Following the same method, commercial shopping bags were shredded and injection-molded into tensile test specimens for comparison.

2.3.2 | Disintegration under Industrial Composting Conditions

Disintegration tests under aerobic composting conditions were performed on a laboratory scale for 90 days (ISO 20200:2015). Blown films of PBSA and P70-T30 were cut into squares (25 mm x 25 mm x 0.1 mm), which were weighed and placed in a textile mesh to ease their withdrawal during composting and to allow access to moisture and microorganisms. The specimens were buried at a depth of 4–6 cm in perforated plastic boxes containing a solid synthetic wet waste (10 wt.% of compost, 30 wt.% rabbit food, 10 wt.% starch, 5 wt.% sugar, 4 wt.% corn oil, 1 wt.% urea, 40 wt.% sawdust and extra 50 wt.% of water) and were incubated under aerobic conditions at 58°C guaranteed by periodic mixing of the solid synthetic wet waste. Samples of each formulation were withdrawn from the disintegration container at different times, cleaned with distilled water, dried in an oven at 50°C for 24 h, and weighed. The mass loss was calculated with respect to the initial weight.

2.4 | Characterization Methods

Tensile tests were performed on dumbbell-shaped specimens (gauge length of 25 mm) cut from extruded flat sheets with a manual cutting press (Elastocon EP 08). The recycled materials were instead tested on injection-molded samples with the same gauge length. Before testing, the samples were conditioned for 48 h at 23°C and 53% relative humidity (RH%) using a closed chamber with saturated $Mg(NO_3)_2$ salt solution. Three specimens for each material and the recycled samples were tested according to the standard ASTM D638-14. A Zwick Z 2.5 Instron machine (ZwickRoell Ltd., Leominster, UK), equipped with a load cell of 2 kN, was operated at a crosshead speed of 10 mm min^{-1}.

Dynamic Mechanical Thermal Analysis (DMTA) tests were carried out with a DMA Q800 (TA Instruments, New Castle, DE, USA) apparatus in tension-film mode on rectangular bars with a width of 10 mm and a length of 16 mm cut from the extruded flat sheets. Before testing, the samples were conditioned for 48 h at 23°C and 53 RH%. The temperature range of the test was from −65 to 70°C with a heating rate of 3°C min^{-1} and a frequency of 1 Hz. The glass transition temperatures (T_g) were determined as the temperatures of the peaks of tanδ, and the damping factor (DF) as the maximum value of tanδ.

The morphological characterization was performed by scanning electron microscopy (SEM) on cryo-fractured samples in liquid nitrogen. The surface of the samples recovered from the compost was also analyzed. Before microscopic analysis, the samples were gold-coated using a sputter coater at 1.5 kV and 10 mA for 50 s. The surface was then investigated with an Ultra 55 FEG SEM (Zeiss Sigma).

Number average molecular weight (M_n), weight average molecular weight (M_w), and polydispersity index (Đ) of PBSA before and after mechanical recycling were determined by gel permeation chromatography (GPC) performed in $CHCl_3$ at ambient temperature, using an HP 1100 Series equipped with a PL gel 5 µm Minimixed-C column and a refractive index detector. Polystyrene standards were used to prepare a universal calibration curve. The detection limit of the column is 500 g mol^{-1}.

Thermal stability was studied by thermogravimetric analysis (TGA) with a Mettler Toledo TGA/DSC3+. Approximately 5 mg of each sample were preheated from room temperature to 70°C, where an isothermal segment was maintained for 15 min to remove residual moisture. Then the samples were heated to 500°C at a heating rate of 5°C min^{-1} under N_2 constant flow of 50 mL min^{-1}. The onset of degradation (T_{onset}) was defined as the temperature at which the sample lost 5% of its initial mass. The degradation temperatures (T_d) were selected as the peak of the first-order derivative. The char residue is the residual mass at 500°C.

DSC analysis was performed on a Mettler Toledo DSC2. The heating/cooling/heating scans were recorded from -80°C to 180°C, at a rate of 10°C min^{-1}, under N_2 constant flow of 50 mL min^{-1}. Native starch was tested under the same conditions but with a 50°C min^{-1} heating rate. The crystallinity (χ_c) of PBSA was computed according to equation (1):

$$\chi_c = \frac{\Delta H_m}{\Delta H^0_{PBSA} * f} * 100 \quad (1)$$

where ΔH_m is the melting enthalpy of the studied sample, ΔH^0_{PBSA} is the melting enthalpy of perfectly crystalline PBSA (142 J g^{-1} [20]), and f is the mass fraction of PBSA in the sample.

Attenuated total reflection Fourier transform infrared (ATR-FTIR) spectra of the samples extracted from compost were acquired with a PerkinElmer FT-IR Spectrometer Frontier in ATR mode. 32 scans were performed from 4000 to 400 cm^{-1} with a resolution of 4 cm^{-1}. All data were treated using the PerkinElmer Spectrum software.

3 | Results and Discussion

3.1 | Extrusion of Blends and Their Properties

Starch has a narrow thermal stability and processing window, highly sensitive to water content. Therefore, plasticization of starch requires careful control of key parameters, including temperature, shear stress, and moisture content, which can significantly impact the viscosity of the system. At low temperatures and shear stresses, incomplete gelatinization may result in residual crystallinity, which can negatively impact processability. On the other hand, higher extrusion temperatures increase the risk of thermo-mechanical degradation of starch and the formation of voids within the material structure [21]. An appropriate moisture content can reduce the system's viscosity during plasticization, thus mitigating thermal degradation. However, this comes at the cost of process efficiency, as energy is lost through water evaporation.

In this study, PBSA/TPS blends were produced using two different melt processing approaches: (i) plasticizing starch in a twin-screw extruder followed by compounding with PBSA in a single-screw extruder, and (ii) a direct one-step extrusion process using the SSE. The objective was to evaluate the effectiveness of stable starch plasticization while maintaining the equilibrium moisture content of potato starch, eliminating the need for a time-consuming and energy-intensive pre-drying step.

In the two-step process, TPS was successfully produced using a co-rotating TSE and subsequently compounded with PBSA in the SSE equipped with a flat die. This setup allowed for both melt compounding and shaping in a single piece of equipment, producing materials suitable for further testing. In the one-step method, native starch, glycerol, water, and PBSA were fed simultaneously into the SSE. As a result, starch plasticization, blending with PBSA, and film shaping occurred in a single, continuous process within the same equipment.

The visual quality of the extruded films differed significantly between the two methods. Films obtained via the two-step process appeared rough, with small visible particles, indicating inhomogeneous mixing. In contrast, films produced using the one-step process exhibited a smooth and homogeneous surface free of visible defects (Figure 1).

DSC analysis revealed that neither the blending method nor the TPS content significantly affected the glass transition temperatures of PBSA (Table S2 and Figure S3). The glass transition of TPS was not detectable by DSC. Two distinct melting peaks associated with the PBSA phase were observed in the two-step samples, suggesting a melting-crystallization-remelting process typical of polyesters. This phenomenon likely arises from the presence of less perfect PBSA crystals formed during the two-step process, whereas the one-step samples exhibited one melting peak, as for neat PBSA.

TGA identified two major degradation temperatures at approximately 300°C and 388°C, corresponding to TPS and PBSA degradation, respectively (Table S2). The degradation temperatures of the blends were unchanged, regardless of TPS content or processing method (Table S2 and Figure S3). However, the onset temperature of degradation decreased with increasing TPS concentration, consistent with the inherently lower thermal stability of TPS compared to PBSA.

DMTA was performed to further assess glass transition temperatures and the thermomechanical properties of the blends. All blends produced by the one-step process showed storage moduli higher than PBSA across the temperature range examined (Figure 2b'). The enhanced stiffness observed in the one-step blends suggests improved stress transfer between the phases, indicative of stronger interfacial interactions between TPS and PBSA in this processing design.

The peak of tanδ, associated with the glass transition, occurs at −38 °C and at 30°C for neat PBSA and neat TPS, respectively (Table 2 and Figure 2a'). In the tanδ plots of the two-step processed blends (Figure 2a), both transitions are clearly identifiable at temperatures close to those of the respective neat polymers, indicating their immiscibility. Both glass transition temperatures slightly decreased with the decreased content of the respective phase. These small shifts suggest limited interaction between the two polymer phases and support the conclusion of inefficient phase mixing, which can hinder effective stress transfer across the interface and negatively impact the mechanical performance of the blends.

The blends produced via the one-step method (Figure 2a') exhibit only a single tanδ peak at approximately -38 °C, corresponding to

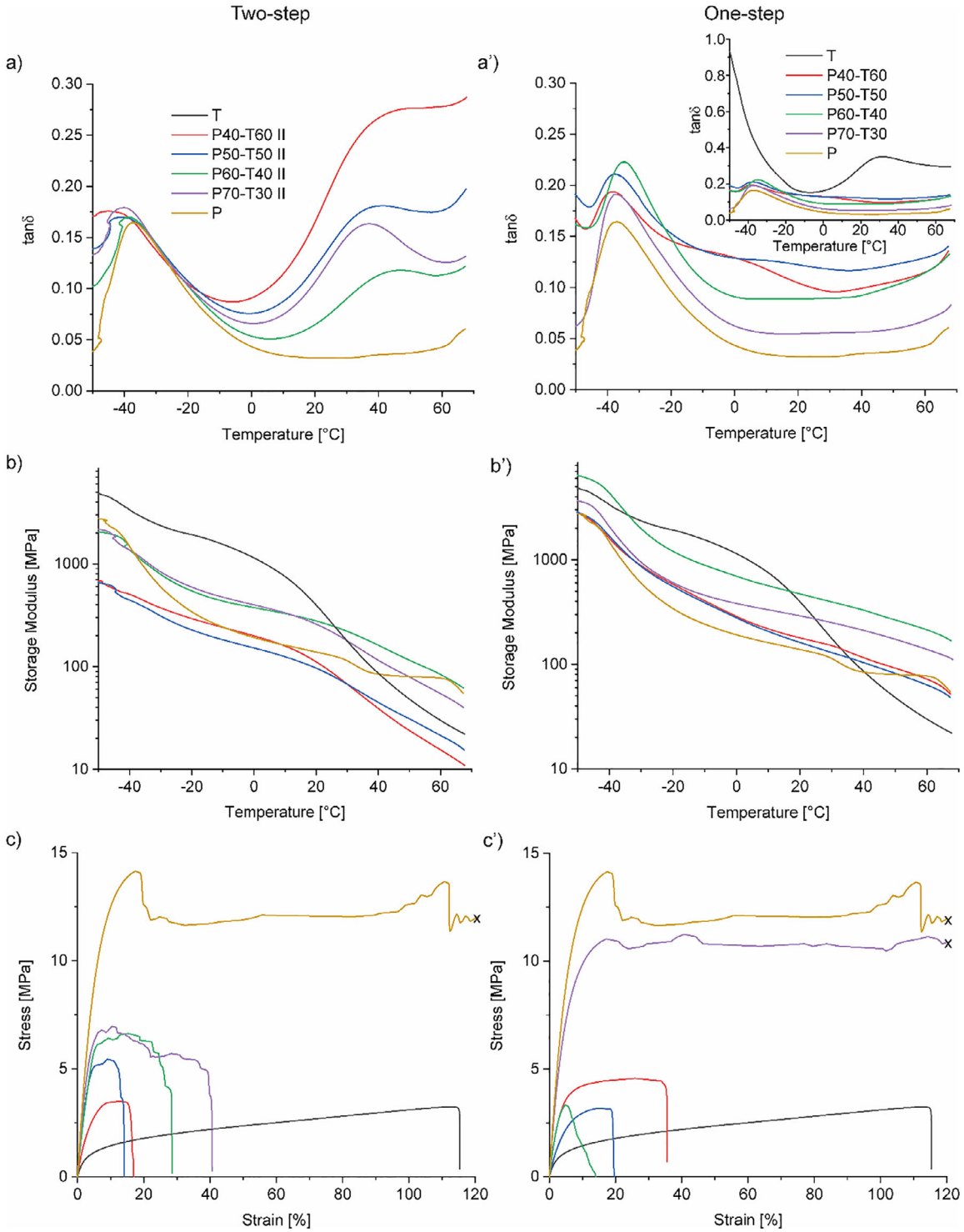

FIGURE 2 | Storage modulus and tanδ recorded by dynamic mechanical thermal analysis in temperature sweeps of the blends in two-step (a) and (b), and one-step (a') and (b'). The inset in b' reports the curves in comparison with that of TPS. Representative tensile curves of the blends prepared in (c) two steps and (c') one step.

the glass transition of the PBSA phase. The glass transition of the TPS phase is not detectable in these samples, and it is accordingly absent in the loss modulus curves (Figure S4). This absence may be attributed to increased miscibility between the two phases or to the presence of residual water retained within the TPS phase, which could broaden and suppress the tanδ peak associated with its glass transition. The damping factor of all materials is below 1 over the entire temperature range, indicating a viscoelastic solid behavior. Neat TPS shows a higher damping factor compared to neat PBSA, consistent with previous observations for similar biopolyesters [22, 23]. This may result from the more amorphous nature of TPS, which facilitates higher energy dissipation than

TABLE 2 | Glass transitions (T_g) and damping factor (DF) measured by tanδ in DMTA. T_{g1} and T_{g2} refer to the glass transition of PBSA and TPS phases, respectively. The values of transitions measured by the loss modulus peak are reported in parentheses. Average tensile properties of the blends with standard deviation: Ultimate tensile strength (UTS), strain at break (ε_b) and Young's modulus (E).

Material	T_{g1} [°C]	T_{g2} [°C]	DF	E [MPa]	UTS [MPa]	ε_b [%]
T	—	30 (19)	0.38	53 ± 4	3 ± 0.2	108 ± 6
P	−38 (−41)	—	0.16	252 ± 4	22 ± 4	590 ± 10
P70-T30 II	−40 (−39)	37 (25)	0.18	190 ± 24	6 ± 1	29 ± 7
P60-T40 II	−41 (−41)	40 (32)	0.17	172 ± 2	6 ± 0.6	31 ± 3
P50-T50 II	−42 (−38)	42 (23)	0.17	165 ± 40	6 ± 0.6	14 ± 5
P40-T60 II	−45 (−40)	44 (23)	0.17	96 ± 8	3 ± 0.3	18 ± 2
P70-T30	−38 (−42)	—	0.19	220 ± 5	15 ± 0.5	444 ± 37
P60-T40	−38 (−39)	—	0.22	132 ± 2	3 ± 0.5	8 ± 0.5
P50-T50	−37 (−40)	—	0.22	77 ± 8	3 ± 0.3	16 ± 3
P40-T60	−37 (−41)	—	0.20	121 ± 10	4 ± 0.5	30±4

the semi-crystalline PBSA. However, the damping factor of all blends is similar and closer to that of neat PBSA, suggesting a more elastic response of the blends compared to TPS alone.

The tensile tests conducted at room temperature (Figure 2c,c') reveal a jagged profile of the curves of the two-step samples, indicating partial premature failures. In these blends, the incorporation of dried TPS led to a progressive reduction in mechanical performance with increasing TPS content compared to neat PBSA (Table 2), despite a slight increase in PBSA crystallinity (Table S2). All blends show significantly lower strain at break than neat PBSA, indicating poor interfacial adhesion and stress transfer between the phases. The P70-T30 blend is an exception, as it retained the deformation and stiffness of the polyester, indicating a more favorable interaction. This is likely due to the lower TPS content and more homogeneous distribution achieved during one-step processing. The PBSA blend with 30 wt.% TPS reported by Wang et al. [13] is characterized by similar tensile strength as the one in this work, but lower deformation (around 325%, compared to 450% of P70-T30). At the same TPS content, Ratto et al. [12] achieved similar deformation and tensile strength values to P70-T30; however, their blend had almost double the stiffness of P70-T30. Given its ability to sustain a high deformation (around 450%), the P70-T30 composition was selected for film blowing to evaluate whether the mixing achieved through one-step processing provided sufficient melt strength for this shaping process.

SEM was performed on cryo-fractured samples to investigate the morphology of the blends in the two methods. In the two-step blends (Figure 3), TPS was not homogeneously distributed within the PBSA matrix; instead, it formed agglomerates with a non-uniform size distribution. This morphological heterogeneity can be attributed to the significant viscosity mismatch between the two components when TPS is introduced in its already plasticized form, as well as to the different polarity of PBSA and TPS. The SEM analysis supports the hypothesis of inefficient mixing in the two-step process, revealing increasing phase debonding with TPS content. These morphological findings are consistent with the observed trends in thermomechanical and tensile properties, further confirming the limitations of the two-step method in achieving effective blend homogeneity.

Neat TPS is characterized by a smooth fracture surface [24], with no apparent phase separation between potato starch and glycerol, confirming homogeneous plasticization (Figure 4a). In the blends produced via the one-step process (Figure 4), the morphology reveals more uniformly distributed phases compared to the two-step samples, characterized by elongated domains and reduced interfacial debonding. This improved dispersion can be attributed to the higher moisture content retained during processing, in contrast to the two-step method, where water is lost through the venting and drying stages. Increasing the water content leads to a reduction in the viscosity of TPS [25], facilitating its dispersion. When water is still present during the blending, the viscosity of TPS is lowered and becomes more similar to that of PBSA. The viscosity matching between the two phases promotes more efficient mixing and better interfacial adhesion [26].

All one-step blends present voids that can be attributed to retained water during processing, given the absence of a venting system in the SSE. As a result, bubbles are observed within the starch-rich phase, with the PBSA phase acting as a sealing layer that inhibits the release of steam. When starch and water are extruded at temperatures above 100 °C, steam expansion occurs as the material exits the die under high-pressure conditions, leading to void formation [27]. Air bubble entrapment during extrusion is also influenced by the barrel filling regime. During the melting process, air initially present in the feed may become trapped and converted into bubbles within the melt. This occurs due to the formation of a fully filled region in the melting zone, which creates a barrier between the feeding and the melting sections. As a result, the air occupying voids during the melting transition cannot escape through the feed port. This entrapment leads to high porosity and a high density of bubbles in the final product. To mitigate this issue, one effective strategy is to maintain the barrel section between the feeder and the melting zone in a starved feeding condition. This approach allows air to escape, reducing bubble formation and improving the morphological quality of the extrudate [28].

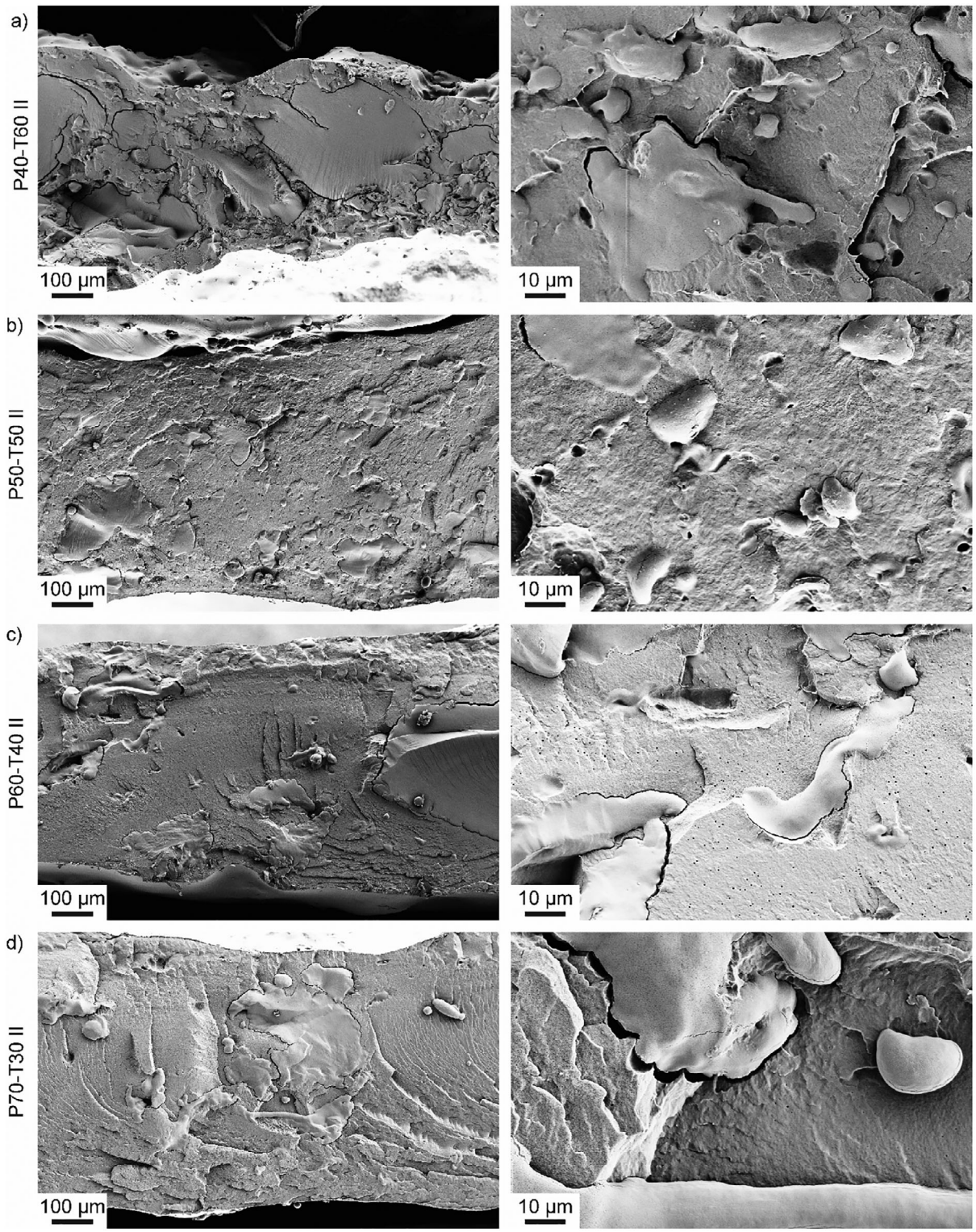

FIGURE 3 | Cryo-fractured surface morphology analysed by scanning electron microscopy of (a) P40-T60 II, (b) P50-T50 II, (c) P60-T40 II, (d) P70-T30 II processed in two steps, with higher magnification (10 µm scale bar) on the right side.

Comparing P70-T30 to P70-T30 II is evident, even at small magnifications, that the former has a smoother surface and the TPS appears homogeneously dispersed as small spherical domains, while in the latter TPS tends to form clusters of different dimensions. As a consequence, the deformation of P70-T30 is more than thirty times that of P70-T30 II. These results highlight that plasticizing the starch simultaneously with the PBSA melting achieves better mixing, leading to improved properties, in addition to the energetic advantage of employing a single step.

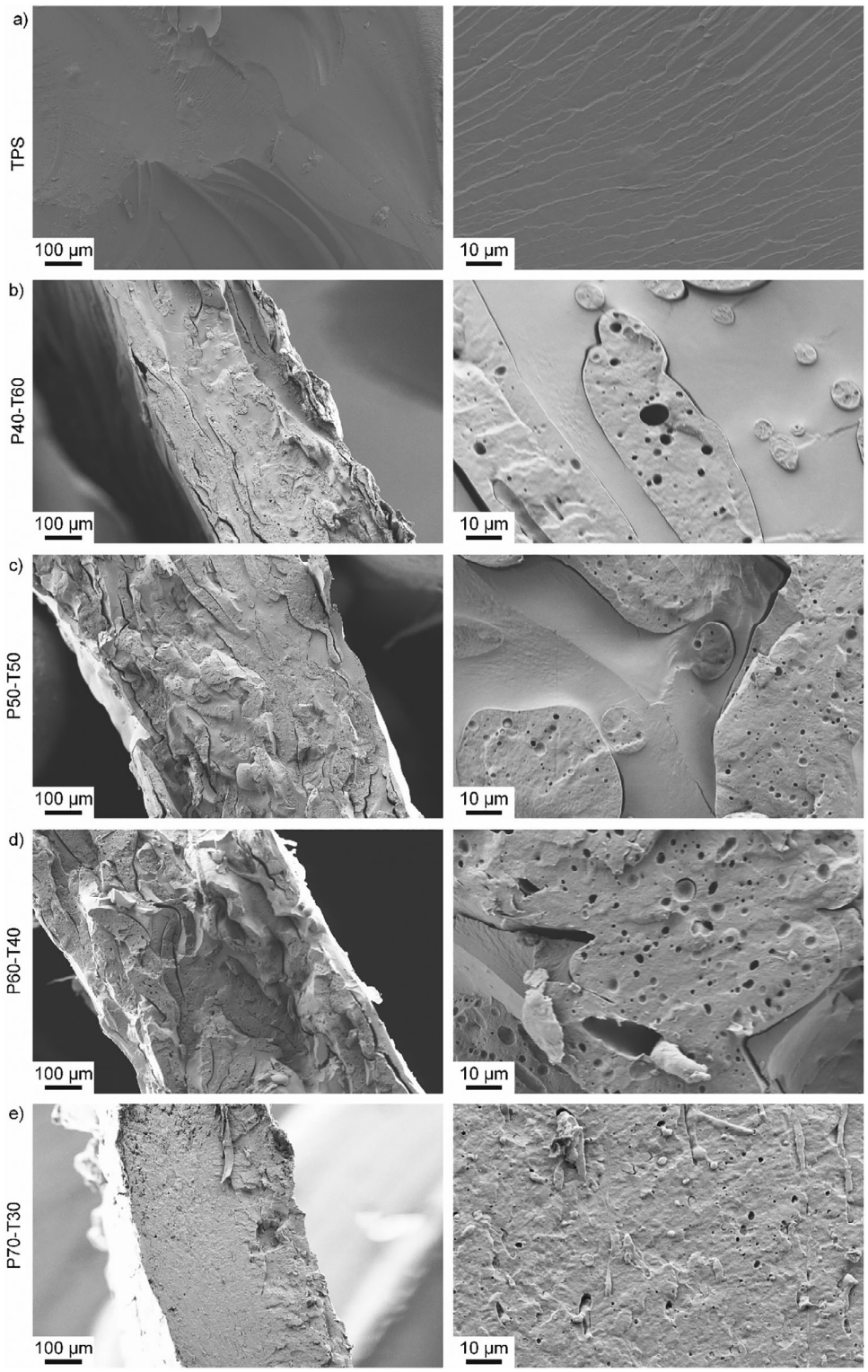

FIGURE 4 | Cryo-fractured surface morphology analyzed by scanning electron microscopy of (a) TPS, (b) P40-T60, (c) P50-T50, (d) P60-T40, (e) P70-T30 processed in one step, with higher magnification (10 µm scale bar) on the right side.

3.2 | Film Blowing and End-of-Life

Film blowing requires that the polymer melt can be stretched without breaking for high-quality film formation. Neat PBSA was used as a benchmark and compared with the P70-T30 formulation. The P70-T30 blend was film blown by directly feeding the mix of native starch, glycerol, water, and PBSA. The two-step equivalent of P70-T30 could not be extruded by film blowing, conceivably given the worse mechanical properties observed after film casting (Figure 2c,c'). By comparing the diameter of the film blowing die to the diameters of the extruded bubbles, the resulting blow-up ratios were 6 to 7 for neat PBSA and 3,2 to 4,2 for P70-T30.

Both materials (Figure 5a) could undergo stable film blowing; however, the starch blend was less stretchable in the transverse direction compared to neat PBSA. The results confirmed the successful and stable film blowing of the P70-T30 blend prepared in one step, demonstrating its ability to meet the mechanical and rheological demands of this processing technique. This finding supports the potential application of the developed bio-based and biodegradable blend for packaging purposes.

After one year of storage, the PBSA and P70-T30 blown films were shredded and injection-molded to produce specimens for tensile tests (Figure 5b). The mechanical analysis shows similar stiffness and strength between PBSA and P70-30 (Table S3), but lower deformation for the starch blend (around 700% and 450% for PBSA and P70-30, respectively). To assess the suitability of these materials for commercial use, shopping bags available in supermarkets in Italy and Sweden were used as benchmarks (Table S4). The commercial bags are based on polyethylene, a biodegradable polyesters blend, and two starch-based blends; however, the exact composition is unknown. The P70-30 sample falls in the same range of stiffness and tensile strength as the polyethylene and the starch-based shopping bags, while the biodegradable polyesters blend has a lower Young's modulus. In terms of deformation, P70-30 is comparable to the commercial starch blends, while it has double the elongation at break of the tested polyethylene. In light of these results, it can be concluded that the blends produced in this work are comparable to some of the existing fossil-based (polyethylene) and biodegradable materials currently used for commercial applications such as shopping bags.

Considering potential industrial applications, it is essential to explore sustainable end-of-life strategies. For this reason, the blown films of both neat PBSA and the P70-T30 blend were subjected to simulated post-industrial mechanical recycling and industrial composting, in order to evaluate their recyclability and biodegradability under controlled conditions.

PBSA and P70-T30 films were re-extruded for four cycles, followed by injection molding and subsequent testing after the first and fourth cycles. Both materials exhibited noticeable darkening after the fourth reprocessing cycle, with the P70-T30 blend showing a more pronounced color change (Figure 5b). This discoloration suggests the occurrence of thermal oxidative degradation induced by the combined effects of extrusion shear forces and processing temperatures [29, 30]. The molecular weight of PBSA before and after recycling was measured to assess potential degradation (Table S5). The blend was excluded from this analysis due to difficulties in solubilizing the TPS phase. After four reprocessing cycles, a decrease in both M_n and M_w was observed, indicating polymer chain scission as a result of thermomechanical degradation during extrusion. Thermal characterization of the recycled samples was performed by DSC and TGA (Table S2). No significant changes were detected in the thermal transition or degradation temperatures after recycling, despite the reduced molecular weight of PBSA. These findings demonstrate that multiple extrusion cycles are feasible without inducing significant thermo-oxidative degradation in PBSA.

Tensile testing of the injection-molded recycled materials showed no significant variation in the mechanical properties of PBSA after recycling (Figure 5c and Table S3). The P70-T30 blend exhibited an improvement in ultimate tensile strength and strain at break after the first recycle. This enhancement can be attributed to improved dispersion and mixing of PBSA and TPS during the second extrusion, which possibly reduced the size of starch granules that typically act as stress concentrators and premature failure sites. After four cycles, a slight decline in tensile properties was observed. Overall, thermal and mechanical characterizations demonstrated that both neat PBSA and the P70-T30 blend can be reprocessed multiple times with minimal loss of performance, supporting their suitability for circular applications.

Weight loss during composting is a key parameter for determining the biodegradation of a material. To evaluate this, blown films of neat PBSA and the P70-T30 blend were tested in industrial composting for 90 days, with periodic mass measurements according to ISO 20200:2015. Both materials achieved over 90% weight loss by the end of the testing period, though they exhibited distinct disintegration kinetics (Figure 5d,e). The starch-containing P70-T30 blend disintegrated significantly faster, reaching 90% weight loss within 42 days, compared to 60 days needed for neat PBSA. This accelerated degradation of the blend aligns with previously reported results for TPS-biopolyester systems, where starch promoted earlier fragmentation and microbial activity, thus enhancing the overall disintegration rate [23, 31]. After 7 days, PBSA had minimal weight loss while the blend reached around 15% weight loss due to the early degradation of starch both by hydrolysis and microorganisms' activity. A similar activation time for PBSA biodegradation was also reported in the literature [32].

The surface morphology of the neat PBSA and P70-T30 films was examined by SEM before composting and after 7 and 14 days in industrial composting (Figure 6). In the case of the P70-T30 blend, degradation occurred primarily through surface pitting, with visible holes forming in correspondence with TPS-rich regions, suggesting that TPS agglomerates acted as initiation sites for microbial attack and biodegradation. The PBSA films exhibited a more uniform surface degradation. The disintegration of PBSA is likely driven by the preferential hydrolysis of its amorphous regions, resulting in an increased relative crystallinity. This process can increase the brittleness of the material, facilitating the fragmentation and further biodegradation [33]. The micrographs of both materials on day 14 revealed the presence of different types of microorganisms, rounded and elongated, confirming the microbial presence during the composting.

ATR-FTIR was employed to assess chemical changes in the films during compost at 0, 7, and 14 days (Figure S5). The spectrum of neat PBSA remained unchanged after 7 days. After 14 days, a broad absorption band emerged around 3200 cm^{-1}, attributed to hydroxy groups. This indicates the hydrolysis of ester bonds, resulting in the formation of alcohol and carboxylic acid end-groups. For the P70-T30 blend, the broad peak at 3200 cm^{-1} was already present prior to composting, due to the inherent hydroxy groups of the starch. This peak significantly diminished after 7 days, suggesting rapid biodegradation of the starch fraction at the surface. By day 14, a re-emergence of the hydroxy band was observed, likely due to the hydrolytic degradation of the PBSA phase, similar to what was seen in the neat PBSA sample.

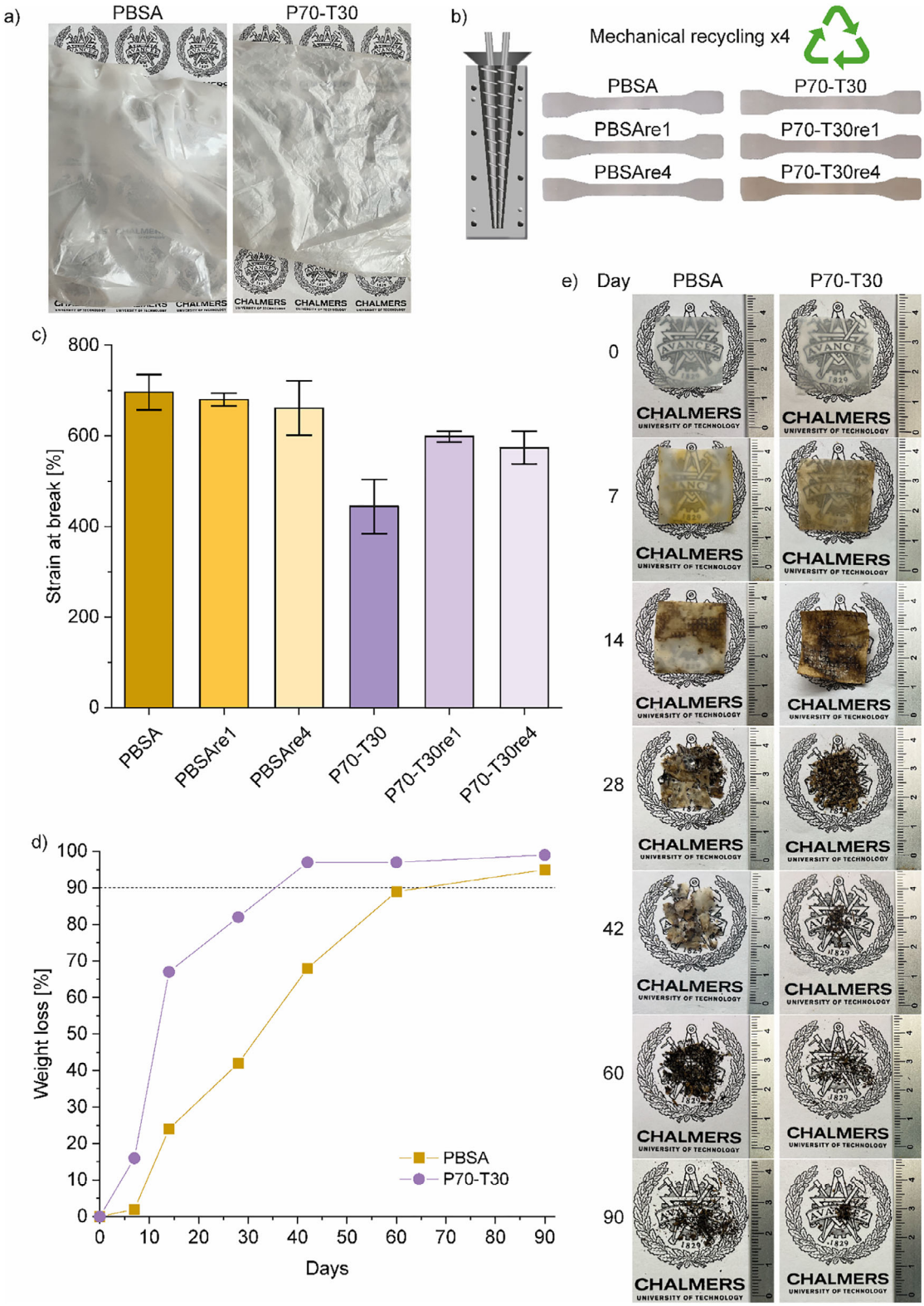

FIGURE 5 | (a) Photographs of blown films of PBSA and P70-T30. (b) Simulation of post-industrial mechanical recycling of PBSA and P70-T30 with photographs of tensile specimens after one year of aging and after 1 or 4 reprocessing cycles. (c) Tensile strain-at-break of the materials before and after recycling. (d) Weight loss during simulation of industrial composting up to 90 days. (e) Photographs of the films withdrawn during industrial composting.

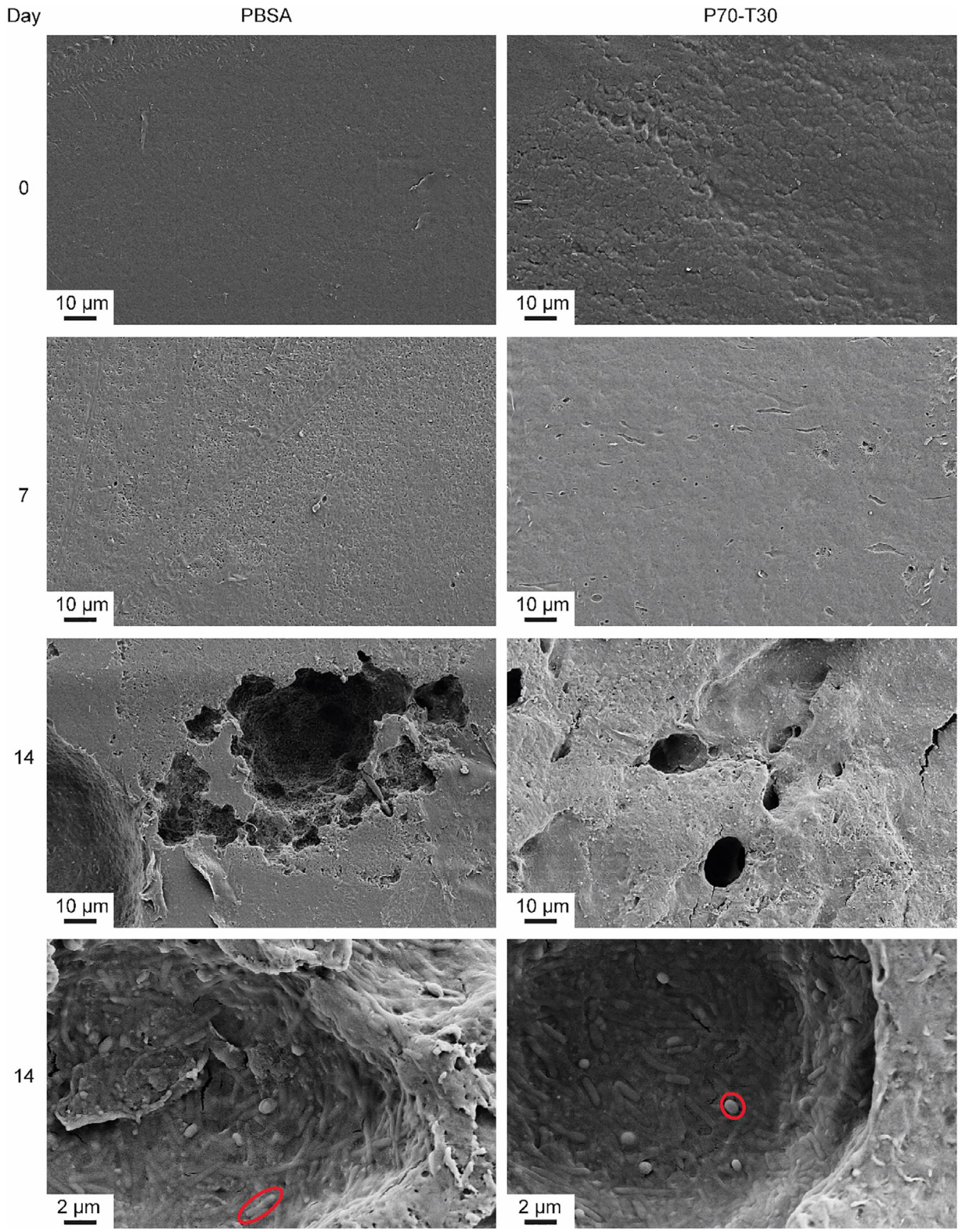

FIGURE 6 | Scanning electron microscopy of PBSA and P70-T30 surfaces at days 0, 7, and 14 of disintegration in compost. The red circles identify examples of microorganisms.

4 | Conclusions

This study aimed to develop bio-based and biodegradable PBSA/TPS blends and to compare two melt extrusion methods: a conventional two-step approach involving starch plasticization followed by blending, and a one-step process that combines plasticization, blending, and shaping. Thermomechanical and morphological analyses demonstrated better performance for the one-step blends. Films produced via the one-step process exhibited smoother, more homogeneous surfaces and a finer dispersion

of TPS domains, as confirmed by SEM. These improvements are attributed to the higher water content retained during the one-step process, which reduces TPS viscosity and facilitates better mixing with PBSA. In contrast, the two-step method, involving drying of TPS before blending, resulted in poor phase dispersion and incomplete melting during re-extrusion. The one-step blends showed better mechanical performance, particularly the P70-T30 composition, which retained a high strain at break (450%). DMTA further supported the enhanced interfacial interaction in the one-step blends, with a higher storage modulus than neat PBSA in the temperature range tested (−50 to 70 °C). The P70-T30 blend was successfully processed via film blowing directly from native starch, glycerol, water and PBSA, confirming the suitability of the one-step process for shaping techniques. To assess end-of-life scenarios, the films were evaluated under simulated post-industrial mechanical recycling and industrial composting. After four extrusion cycles, the P70-T30 blend retained its thermal and mechanical properties, demonstrating good recyclability. In industrial composting, the blend achieved over 90% weight loss within 42 days, significantly faster than neat PBSA, and fulfilled the weight loss limit for industrial composting (EN 13432). In conclusion, the one-step extrusion approach not only simplifies processing and reduces energy input but also yields blends with superior performance and sustainable end-of-life options.

Funding

This work was supported by the Knut and Alice Wallenberg Foundation (KAW) through the Wallenberg Wood Science Center (WWSC 3.0: KAW 2021.0313, project number II-15).

Conflicts of Interest

The authors declare no conflicts of interest.

Data Availability Statement

The data that support the findings of this study are available from the corresponding author upon reasonable request.

References

1. R. Geyer, J. R. Jambeck, and K. L. Law, "Production, Use, and Fate of all Plastics Ever Made," *Science Advances* 3 (2017): 1700782, https://doi.org/10.1126/sciadv.1700782.

2. Plastic pollution is growing relentlessly as waste management and recycling fall short, says OECD, https://www.oecd.org/environment/plastic-pollution-is-growing-relentlessly-as-waste-management-and-recycling-fall-short.htm (accessed January 18, 2024).

3. Market – European Bioplastics e.V., https://www.european-bioplastics.org/market/ (accessed February 6, 2025).

4. G. Z. Yin and X. M. Yang, "Biodegradable Polymers: A Cure for the Planet, but a Long Way to Go," *Journal of Polymer Research* 27 (2020): 1–14, https://doi.org/10.1007/s10965-020-2004-1.

5. H. A. Makroo, S. Naqash, J. Saxena, S. Sharma, D. Majid, and B. N. Dar, "Recovery and Characteristics of Starches From Unconventional Sources and Their Potential Applications: A Review," *Applied Food Research* 1 (2021): 100001, https://doi.org/10.1016/j.afres.2021.100001.

6. P. M. Forssell, S. H. D. Hulleman, P. J. Myllärinen A, G. K. Moates, and R. Parker, "Ageing of Rubbery Thermoplastic Barley and Oat Starches," *Carbohydrate Polymers* 39 (1999): 43–51, https://doi.org/10.1016/S0144-8617(98)00128-3.

7. V. Tanrattanakul and W. Panwiriyarat, "Compatibilization of low-density polyethylene/cassava starch blends by potassium persulfate and benzoyl peroxide," *Journal of Applied Polymer Science* 114 (2009): 742–753, https://doi.org/10.1002/app.30659.

8. A. P. Abbott, T. Z. Abolibda, W. Qu, W. R. Wise, and L. A. Wright, "Thermoplastic starch–polyethylene blends homogenised using deep eutectic solvents," *RSC Advances* 7 (2017): 7268–7273, https://doi.org/10.1039/C7RA00135E.

9. H. Vieyra Ruiz, E. S. M. Martínez, and M. Ã. A. Méndez, "Biodegradability of polyethylene–starch blends prepared by extrusion and molded by injection: Evaluated by response surface methodology," *Starch—Stärke* 63 (2011): 42–51, https://doi.org/10.1002/STAR.201000075.

10. E. Rudnik, "Compostable Polymer Materials," in *Handbook of Biopolymers and Biodegradable Plastics* (Elsevier, 2013), 189–211, https://doi.org/10.1016/B978-1-4557-2834-3.00010-0.

11. X.-L. Wang, K.-K. Yang, and Y.-Z. Wang, "Properties of Starch Blends With Biodegradable Polymers," *Journal of Macromolecular Science, Part C: Polymer Reviews* 43 (2003): 385–409, https://doi.org/10.1081/MC-120023911.

12. J. A. Ratto, P. J. Stenhouse, M. Auerbach, J. Mitchell, and R. Farrell, "Processing, Performance and Biodegradability of a Thermoplastic Aliphatic Polyester/Starch System, Polymer (Guildf)," *Polymer* 40 (1999): 6777–6788, https://doi.org/10.1016/S0032-3861(99)00014-2.

13. Y. Wang, Y. Zhong, Q. Shi, and S. Guo, "Study of the Preparation and Properties of TPS/PBSA/PLA Biodegradable Composites," *Journal of Composites Science* 5 (2021): 48, https://doi.org/10.3390/jcs5020048.

14. R. P. H. Brandelero, M. V. E. Grossmann, and F. Yamashita, "Effect of the Method of Production of the Blends on Mechanical and Structural Properties of Biodegradable Starch Films Produced by Blown Extrusion," *Carbohydrate Polymers* 86 (2011): 1344–1350, https://doi.org/10.1016/j.carbpol.2011.06.045.

15. C. Noomhorm and Y. Tokiwa, "Effect of Poly(dioxolane) as Compatibilizer in Poly(ε-caprolactone)/Tapioca Starch Blends," *Journal of Polymers and the Environment* 14 (2006): 149–156, https://doi.org/10.1007/s10924-006-0014-7.

16. J. J. M. Swinkels, "Composition and Properties of Commercial Native Starches," *Starch—Stärke* 37 (1985): 1–5, https://doi.org/10.1002/star.19850370102.

17. V. Sessini, H. Latty, M. Milazzo, M. Mirkhalaf, and G. Lo Re, "Experiments and Computational Modelling Combined to Shed Light on the Reinforcement Mechanism in Reactive Extruded Pulp Fibres/Starch Biocomposites," *Advanced Composites and Hybrid Materials* 8 (2025): 365, https://doi.org/10.1007/S42114-025-01460-5.

18. A. Venkatesh, L. Forsgren, A. Avella, et al., "Water-assisted melt processing of cellulose biocomposites With poly(ε-caprolactone) or poly(ethylene-acrylic acid) for the production of carton screw caps," *Journal of Applied Polymer Science* 139 (2021): 51615, https://doi.org/10.1002/APP.51615.

19. J. J. G. van Soest, K. Benes, D. de Wit, and J. F. G. Vliegenthart, "The Influence of Starch Molecular Mass on the Properties of Extruded Thermoplastic Starch," *Polymer (Guildf)* 37 (1996): 3543–3552, https://doi.org/10.1016/0032-3861(96)00165-6.

20. M. Coltelli, L. Aliotta, G. Fasano, et al., "Recyclability Studies on Poly(lactic acid)/Poly(butylene succinate- co -adipate) (PLA/PBSA) Biobased and Biodegradable Films," *Macromolecular Materials and Engineering* 308 (2023): 2300136, https://doi.org/10.1002/mame.202300136.

21. M. Thuwall, A. Boldizar, and M. Rigdahl, "Extrusion Processing of High Amylose Potato Starch Materials," *Carbohydrate Polymers* 65 (2006): 441–446, https://doi.org/10.1016/j.carbpol.2006.01.033.

22. X. Zhai, W. Wang, H. Zhang, Y. Dai, H. Dong, and H. Hou, "Effects of High Starch Content on the Physicochemical Properties of Starch/PBAT Nanocomposite Films Prepared by Extrusion Blowing," *Carbohydrate Polymers* 239 (2020): 116231, https://doi.org/10.1016/j.carbpol.2020.116231.

23. M. Nevoralová, M. Koutný, A. Ujčić, et al., "Structure Characterization and Biodegradation Rate of Poly(ε-caprolactone)/Starch Blends," *Frontier Material* 7 (2020): 487523, https://doi.org/10.3389/fmats.2020.00141.

24. K. Kaewtatip and J. Thongmee, "The Effects of Cross-linked Starch on the Properties of Thermoplastic Starch," *Materials & Design* 45 (2013): 586–589, https://doi.org/10.1016/j.matdes.2012.09.039.

25. J. L. Willett, B. K. Jasberg, and C. L. Swanson, "Rheology of Thermoplastic Starch: Effects of Temperature, Moisture Content, and Additives on Melt Viscosity," *Polymer Engineering & Science* 35 (1995): 202–210, https://doi.org/10.1002/pen.760350214.

26. P. Pötschke and D. R. Paul, "Formation of Co-continuous Structures in Melt-Mixed Immiscible Polymer Blends," *Journal of Macromolecular Science, Part C: Polymer Reviews* 43 (2003): 87–141, https://doi.org/10.1081/MC-120018022.

27. N. Soykeabkaew, C. Thanomsilp, and O. Suwantong, "A Review: Starch-based Composite Foams," *Composites Part A: Applied Science and Manufacturing* 78 (2015): 246–263, https://doi.org/10.1016/j.compositesa.2015.08.014.

28. F. H. Cisneros and J. L. Kokini, "A Generalized Theory Linking Barrel Fill Length and Air Bubble Entrapment During Extrusion of Starch," *Journal of Food Engineering* 51 (2002): 139–149, https://doi.org/10.1016/S0260-8774(01)00050-4.

29. A. Cascales, C. Pavon, S. Ferrandiz, and J. López-Martínez, "Evaluation of Thermoplastic Starch Contamination in the Mechanical Recycling of High-Density Polyethylene," *Recycling* 9 (2024): 33, https://doi.org/10.3390/recycling9030033.

30. M. Coltelli, L. Aliotta, G. Fasano, et al., "Recyclability Studies on Poly(lactic acid)/Poly(butylene succinate- co -adipate) (PLA/PBSA) Biobased and Biodegradable Films," *Macromolecular Materials and Engineering* 308 (2023): 2300136, https://doi.org/10.1002/mame.202300136.

31. P. C. Mayekar, W. Limsukon, A. Bher, and R. Auras, "Breaking It down: How Thermoplastic Starch Enhances Poly(lactic acid) Biodegradation in Compost—a Comparative Analysis of Reactive Blends," *ACS Sustainable Chemistry & Engineering* 11 (2023): 9729–9737, https://doi.org/10.1021/acssuschemeng.3c01676.

32. R. Altieri, M. Seggiani, A. Esposito, P. Cinelli, and V. Stanzione, "Thermoplastic Blends Based on Poly(Butylene Succinate-co-Adipate) and Different Collagen Hydrolysates From Tanning Industry—II: Aerobic Biodegradation in Composting Medium," *Journal of Polymers and the Environment* 29 (2021): 3375–3388, https://doi.org/10.1007/s10924-021-02124-3.

33. M. Puchalski, G. Szparaga, T. Biela, A. Gutowska, S. Sztajnowski, and I. Krucińska, "Molecular and Supramolecular Changes in Polybutylene Succinate (PBS) and Polybutylene Succinate Adipate (PBSA) Copolymer During Degradation in Various Environmental Conditions," *Polymers* 10 (2018): 251, https://doi.org/10.3390/polym10030251.

Supporting Information

Additional supporting information can be found online in the Supporting Information section.

Supporting File: mame70284-sup-0001-SuppMat.pdf.